9th Asia-Pacific Conference on Wind Engineering
Auckland, New Zealand
3-7 December 2017

Experimental Study of Wind Load of Solar Trackers on Flat-Roof Buildings

Chia-Ren Chu[1], and Sheng-Jue Tsao[1]
[1]Department of Civil Engineering
National Central University, Taiwan 320, R.O.C.

Abstract

This study uses wind tunnel experiment to investigate the aerodynamic loading on the solar tracker installed on flat-roof buildings. The surface pressures on the model tracker are measured under different wind directions, azimuth angles, inclined angles and pedestal height of the tracker. The experimental results reveal that the maximum positive net pressure occurs when wind direction $\theta = 45^o$, while the maximum suction (negative net pressure) occurs when $\theta = 225^o$ for azimuth angle $\alpha = 45^o$ and the absolute value of the maximum suction is greater than the maximum positive pressure for the same tracker height and inclined angle. In addition, due to the separation shear layer on the building roof, the wind load decreases as the tracker height decreases. The surface pressures of the tracker installed on the downwind building of two adjacent buildings are also examined. Due to the shelter effect of upwind building, the windward pressure of the tracker on the roof of downwind building is reduced when the spacing between two buildings is less than five times of building height.

Introduction

Solar collectors installed on the building roofs have the advantage of acquiring the solar energy close to the energy user and require no additional land for the collectors. However, the high wind speed on the building roofs may cause damage to the solar collectors, especially in the typhoon-prone areas like Taiwan. Therefore, the wind loads of the solar collectors installed on the building roofs are of great interest to the engineers. Kopp and Banks [3] indicated that the wind load of the solar collectors is dependent on the building configuration, roof slope, tilted angle of the collector, row spacing, collector height, parapet height and the offset from the leading edge of the building roof.

Most previous studies used wind tunnel experiments to determine the force coefficients of the solar collectors. For example, Radu et al. [5] experimentally investigated the wind pressure of solar panels on flat-roof buildings. Their results revealed that the wind load is significantly reduced by the sheltering effects of the first row of panels and of the building itself. Peterka et al. [4] studied the mean and peak wind loads on rectangular or circular heliostats on the ground in a boundary layer wind tunnel. They measured the horizontal and vertical forces, moments about horizontal and vertical axes of the heliostat. Their results showed that the wind load is higher than predicted from results obtained in a uniform, low-turbulence flow due to the presence of turbulence.

Meroney and Neff [2] used wind tunnel experiments and Computational Fluid Dynamics models to explore the wind load on the photovoltaic (PV) modules on a tilted roof in the wind direction 0^o and 180^o. They found that the RNG k-ε and k-omega turbulence model provided a reasonable agreement with the measured wind loads, whereas the standard k-epsilon model failed to replicate experimental results. Banks [1] experimentally investigated the wind pressure on the solar panels on flat-roof building. They found that, due to the conical vortices on the building roof, the solar panel experienced the maximum positive lift when the wind direction is 45^o, and the negative lift (downward force) on the panel will reach its maximum value when the wind direction is 135^o.

Stathopolous et al. [6] used wind tunnel experiments to examine the influences of the building height, location, inclination angle and wind direction on the peak pressures and force coefficients of the solar panels installed on flat building roofs. Their results revealed that the effect of building height on the wind load of solar panel is minimal, whereas the corner panels are subjected to higher net pressures.

The above studies investigated the solar panels that are parallel to the edges of the building roofs (the azimuth angle between the solar collector and the roof edge $\alpha = 0^o$). However, the azimuth angle of the solar trackers and wind direction will change over time. The conical vortices on the building roof may generate considerable wind load on the solar tracker when $\alpha \neq 0^o$. There is a need to study the influences of the azimuth angle on the wind loads of solar trackers on rooftops, especially the pitching and yawing moments for the tracker. This study investigates the aerodynamic loading of the tracker installed on flat-roofed buildings. A series of wind tunnel experiments were carried out to study the influences of wind direction, azimuth angle and pedestal height on the force coefficients of the solar tracker.

Experimental setup

The experiments were conducted in a suction-type, open circuit wind tunnel. The total length of the wind tunnel is 30 m, and the test section is 18.5 m long, 3.0 m wide and 2.1 m high. A rectangular-shape building model of the height H = 0.6 m, width W = 0.3 m and length L = 0.3 m was placed on the centerline of the test section of the wind tunnel. The approaching flow was a boundary layer flow, generated by the spires and roughness elements placed on the floor of the test section. A scale-down rectangular tracker model (Length Ls = 75 mm, width Ws = 125 mm and thickness 2 mm) was installed at the center of the building roof (see Figure 1). The scale ratio of the tracker is 1:40, and the aspect ratio Ws/Ls = 1.67. The inclined angle of the tracker model was fixed at $\beta = 23^o$, according to the latitude of northern Taiwan. The offset from the leading edge of the roof to the support of the tracker model was 0.15 m. In this study the wind direction θ and the azimuth angle α of the tracker model can be adjusted independently. Three different support heights: h_s = 15, 22 and 32 mm were conducted in the experiment (see Figure 2). Therefore, the ground clearance from the lower edge

of the tracker to the building roof were h_c = 0, 7 and 17 mm, respectively. The maximum blockage ratio of the building and the tracker in the wind tunnel was 3.10%.

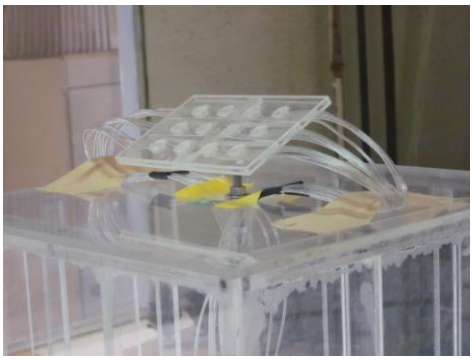

Figure 1. Photograph of solar tracker on building roof.

There were 12 pressure taps (vertical spacing 20 mm and horizontal spacing 25 mm) flush to the tracker model. The pressures were measured by a multi-channel, high-speed pressure scanner (ZOC33/64PX, Scanivalve Inc.). The measuring range of the pressure sensor was ± 2758 Pa, with a resolution of ±2.2 Pa. The sampling frequency was 250 Hz, the sampling duration was 65.53 sec. The pressure module was placed inside the scale model with short tubings (length 0.3 m) connected to the pressure taps. This arrangement guaranteed the high frequency response of the pressure measurement.

The pressure coefficient is defined as:

$$C_p = \frac{P - P_o}{0.5\rho U_H^2} \quad (1)$$

where P is the measured pressure on the model surface, P_o is the reference pressure well above the building, U_H is the undisturbed wind speed at the roof height, ρ is the density of the air. The aerodynamic force of the tracker can be calculated from the pressure distribution on the upper and lower sides of the tracker. The spatial average pressure coefficient C_p is calculated as:

$$\overline{C_p} = \frac{\sum_{i=1}^{12} C_{pi} \times A_i}{\sum_{i=1}^{12} A_i} \quad (2)$$

where C_{pi} is the time-averaged pressure coefficient of i-th pressure tap; A_i is the area around i-th pressure tap. The net pressure coefficient C_{pn} of the tracker is defined as:

$$C_{pn} = \overline{C_{pu}} - \overline{C_{pl}} \quad (3)$$

where C_{pu} and C_{pl} is the area-averaged pressure coefficients on the upper and lower sides of the tracker, respectively. Based on the net pressure coefficient, the drag and lift coefficients can be calculated as:

$$C_D = |C_{pn}| \times \sin\beta \quad (4)$$

$$C_L = -C_{pn} \times \cos\beta \quad (5)$$

where β is the inclined angle of the tracker. The optimal inclined angle of the solar tracker to capture the solar energy is dependent on the latitude and the solar angle.

Results and Discussion

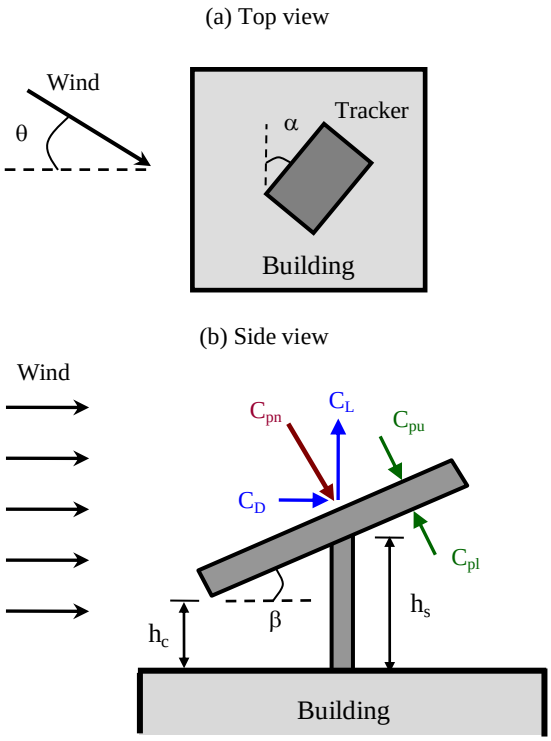

Figure 2. Schematic diagram of a solar tracker on building roof. (a) top view; (b) side view.

Azimuth Angle

This section presents the measured pressure coefficients of the solar tracker under different azimuth angles. The wind direction was fixed θ = 0° (normal to the windward façade of the building). The height of the parapet h_p = 0 and the inclined angle β = 23°. The azimuth angle was varied in the range of α = 0° ~ 180° for every 22.5°. Figure 3 shows the net pressure coefficient and force coefficient. For pedestal height h_s = 15 mm, the values of C_{pu} and C_{pl} were around -0.60 and did not change significantly with the azimuth angle. This led to the net pressure coefficient C_{pn} close to zero, regardless of the azimuth angle. This was owing to the tracker was within the separation shear layer on the building roof when h_s = 15 mm, and the shear layer reduced the wind speed and the influence of azimuth angle on the wind load. For pedestal height h_s = 22 mm and 32 mm, the net pressure coefficient, C_{pn}, was positive when the azimuth angle α < 90°, since the wind was coming from the upper side of the tracker. The net pressure coefficient became negative, C_{pn} < 0, and the tracker experienced an uplift force when α > 90°.

The lift coefficient C_L shown in Figure 3(b) indicates that the highest tracker (h_s = 32 mm) has the maximum downward lift (C_L = -0.40) when the azimuth angle α = 0° (wind direction was normal to the tracker). The maximum lift coefficient C_L = 0.20 occurred when the azimuth angle α = 180° (wind was directly coming from the lower side of the tracker). The drag coefficient (see Figure 3(c)) was smaller than the absolute value of the lift coefficient, since the inclined angle was only 23°.

Wind Direction

In order to examine the effect of wind direction on the wind load of the tracker, the azimuth angle was fixed as α = 0° and 45°, while the wind direction θ was varied in the range of 0° ~ 180°.

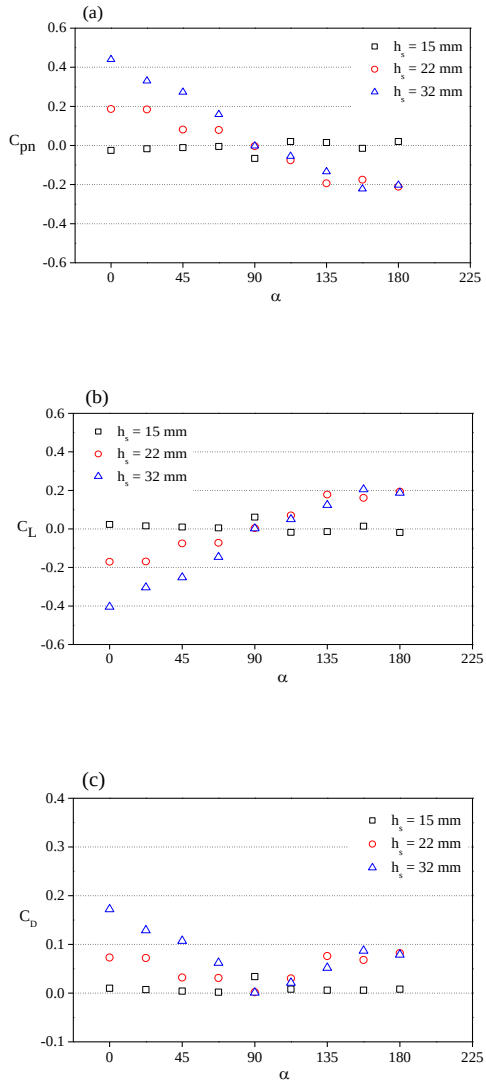

Figure 3. Relationship between azimuth angle and pressure coefficients for different pedestal heights, wind direction θ = 0°. (a) net pressure coefficient; (d) lift coefficient; (e) drag coefficient.

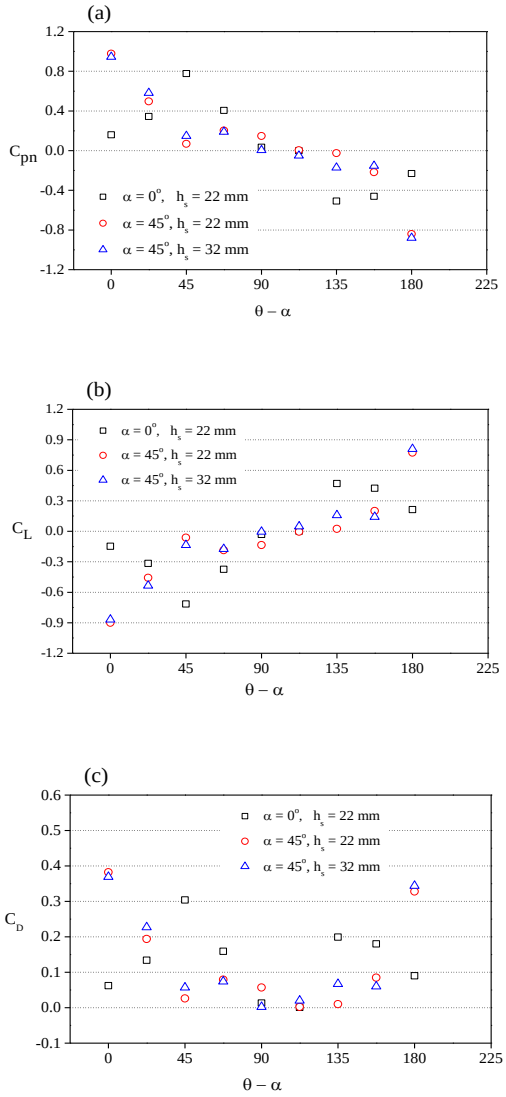

Figure 4. Relationship between relative attack angle and pressure coefficients for azimuth angle α = 0 and 45°. (a) net pressure coefficient; (d) lift coefficient; (e) drag coefficient.

The inclined angle β = 23°, the pedestal height h_s = 22 mm and 32 mm. Figure 4 shows the relationship between the net pressure coefficients and the relative attack angle, θ – α. When the relative attack angle θ – α = 0°, the net pressure coefficient C_{pn} for wind direction θ = 45° and azimuth angle α = 45° was larger than that for θ = 0° and α = 0° (tracker aligned with the building edge), regardless the upper side of the tracker was normal to the wind direction for both cases (see Figure 4(a)). This is due to the corner vortices impact on the tracker when the azimuth angle α = 45°. In addition, the values of net pressure C_{pn} were very close for pedestal height h_s = 22 mm and 32 mm. The maximum net pressure C_{pn} = 0.98 occurred at θ – α = 0°, while the maximum suction C_{pn} = -0.85 occurred at θ – α = 180° (wind was coming from the lower side of the tracker). Also, the variation range of net pressure coefficient C_{pn} (-0.85 ~ 0.98) for α = 45° was larger than the range of C_{pn} (-0.50 ~ 0.80) for α = 0°. Figure 4(b) and 4(c) also indicates that the maximum lift and drag coefficients occurred when the azimuth angle α = 45°.

Effect of Adjacent Building

This study also investigates the effect of adjacent building on the wind load of solar tracker located on the roof of flat-roof buildings. Two flat-roof buildings were placed in tandem arrangement with different spacing S between the buildings (see Figure 5). The solar tracker was located on the roof of the downwind building. The wind direction was θ = 0°, the pedestal height h_s = 22 mm, and the inclined angle β = 23°. The measured pressure coefficients for different dimensionless spacing S^* (= S/H, H is building height) are shown in Figure 6. The solid symbols are tracker on a single building, empty symbols are tracker on downwind building. The shelter effect of upwind building reduced the windward pressure of the solar tracker and lead to larger net pressure C_{pn} when the building spacing $S^* < 5$. The influence of upwind building on the wind load of the tracker became negligible when the spacing $S^* \geq 6$.

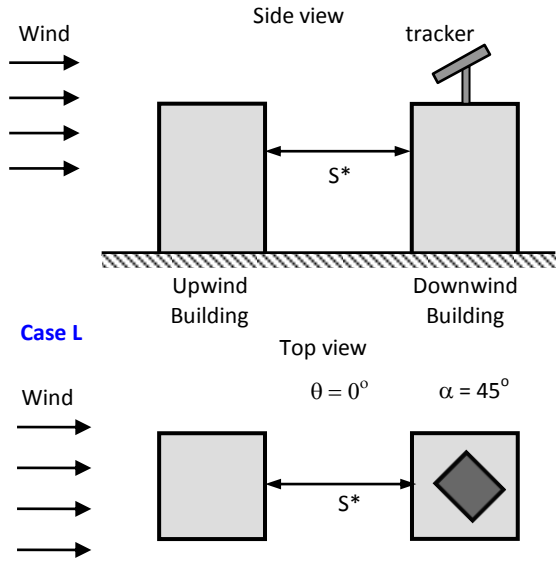

Figure 5. Schematic diagram of two buildings in tandem arrangement.

Conclusions

This study performed a series of wind tunnel experiments to investigate the wind load of solar trackers installed on flat-roof buildings. The pressure distributions of a rectangular solar tracker were measured under different wind directions, azimuth angles and pedestal heights. The experimental results revealed that the relative attack angle between the wind direction and azimuth angle of the tracker is the critical parameter in determining the wind load of the tracker. The maximum wind load occurred when the wind direction $\theta = 45^o$ and azimuth angle $\alpha = 45^o$ (relative attack angle is 0^o). In addition, the magnitude of the area-averaged pressure coefficient increased as the pedestal height increased, regardless of the wind direction and azimuth angle.

For tracker on the downwind building of two adjacent buildings, the shelter effect of upwind building reduced the windward pressure of the solar tracker and lead to larger net pressure when the spacing between two buildings was less than five times of building height. The effect of upwind building on the wind load of the tracker became negligible when the building spacing was greater than six times of building height.

Acknowledgments

The financial support from the Ministry of Science and Technology (MOST), Republic of China, Taiwan, under the grant no. 103-2221-E-008-104 is gratefully appreciated.

References

[1] Banks, D.B. The role of corner vortices in dictating wind loads on tilted flat solar panels mounted on large flat roofs. *J. Wind Eng. Ind. Aerodyn*. **123**, 2013, 192-201.

[2] Meroney, R.N. & Neff, D.E., Wind effects on roof-mounted solar photovoltaic arrays: CFD and wind-tunnel evaluation. *The Fifth International Symposium on Computational Wind Engineering*, Chapel Hill, North Carolina, USA, 2010.

[3] Kopp, G.A. & Banks, D.B., Use of the wind tunnel test method for obtaining design wind loads on roof-mounted solar arrays. *J. Structural Eng.*, ASCE. **139**(2), 2013, 284-287.

[4] Peterka, J.A., Tan, Z., Cermak, J.E. & Bienkiewicz, B. Mean and peak wind loads on heliostats. *J. Solar Energy Eng.*, **111**, 1989, 158-164.

[5] Radu, A., Axinte, E., & Theohari, C., Steady wind pressures on solar collectors on flat-roofed buildings. *J. Wind Eng. Ind. Aerodyn.* **23**, 1986, 249-258.

[6] Stathopoulos, T., Zisis I. & Xypnitou E., Local and overall wind pressure and force coefficients for solar panels. *J. Wind Eng. Ind. Aerodyn.* **125**, 2014, 195-206.

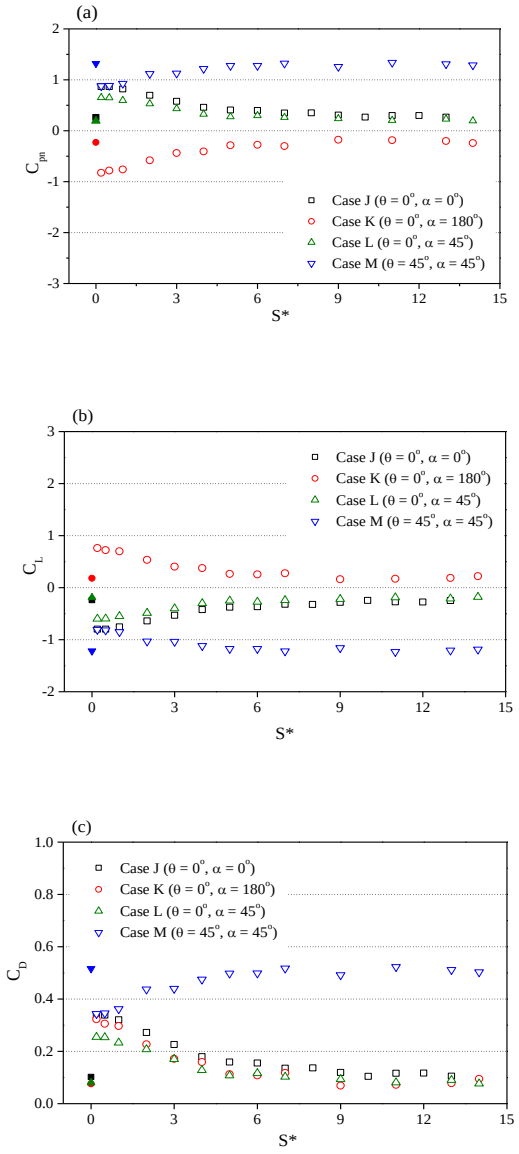

Figure 6. Net pressure coefficient as a function of spacing S^* between two buildings. The solid symbols are the tracker on single building, empty symbols are on downwind building. (a) net pressure coefficient; (b) lift coefficient; (c) drag coefficient.